Talanta 80 (2009) 846–852

Contents lists available at ScienceDirect

Talanta

journal homepage: www.elsevier.com/locate/talanta

Correction of structured molecular background by means of high-resolution continuum source electrothermal atomic absorption spectrometry—Determination of antimony in sediment reference materials using direct solid sampling

Rennan G.O. Araujo[a], Bernhard Welz[a,b,*], Fabiola Vignola[a], Helmut Becker-Ross[c]

[a] Departamento de Química, Universidade Federal de Santa Catarina, 88040-900 Florianópolis - SC, Brazil
[b] INCT de Energia e Ambiente do CNPq, Brazil[1]
[c] ISAS - Institute for Analytical Sciences, Department of Interface Spectroscopy, Albert-Einstein-Str. 9, 12489 Berlin, Germany

ARTICLE INFO

Article history:
Received 28 June 2009
Received in revised form 1 August 2009
Accepted 4 August 2009
Available online 13 August 2009

Keywords:
Antimony determination
Sediment analysis
Direct solid sampling
Electrothermal AAS
High-resolution continuum source AAS

ABSTRACT

A simple, fast and accurate procedure is proposed for the determination of antimony in certified sediment reference materials using direct solid sampling high-resolution continuum source electrothermal atomic absorption spectrometry and iridium as a permanent modifier. The less sensitive resonance line at 231.147 nm has been used in order to allow the introduction of larger sample mass. Six certified reference materials, one river, one estuarine and four marine sediments have been analyzed. The use of iridium as a permanent modifier caused an increase of 30% in sensitivity and stabilized antimony in the sediment to a pyrolysis temperature of 1100 °C. Significant background absorption with pronounced rotational fine structure was observed at the optimum atomization temperature of 2100 °C, which coincided with the analyte atomic absorption in time. This background was found to be due to the electron excitation spectra of mostly the SiO and in part the PO molecules, and could be eliminated by applying a least-squares background correction algorithm. A characteristic mass of 28 pg Sb was obtained, and the limit of detection (3σ, $n=10$) was 0.02 $\mu g\,g^{-1}$, calculated for 0.2 mg of sample. The results obtained for six certified reference materials with concentrations between 0.40 and $11.6 \pm 2.6\ \mu g\,g^{-1}$ Sb were in agreement with the certified values according to a Student's *t*-test for a 95% confidence level, using aqueous standards for calibration. The precision, expressed as relative standard deviation, ranged between 7% and 17% ($n=5$).

1. Introduction

In contrast to other toxic elements, such as arsenic, cadmium, lead or mercury, antimony came into the focus of environmental and health concern only less than a decade ago, maybe because no big environmental accident, such as the Minamata disaster in Japan or the arsenic poisoning in Bangladesh, was associated to antimony intoxication. Antimony and many of its compounds are toxic, bio-accumulative and persistent in the environment and its behavior and transport depend on its chemical form [1–3]. Antimony is generally more toxic than lead due to its higher solubility in lipids, which increases the potential for biological uptake and bio-accumulation. Its presence in the environment is due to natural processes and anthropogenic activities [4–6]. Antimony is increasingly being used in the semiconductor industry, in a wide variety of alloys and as a flame retardant [7,8]. Industries such as smelters, coal-fired plants and refuse incinerators can release relatively high amounts of antimony in the air. When released to air, antimony can attach itself to very small particles and may stay in the atmosphere for many days and be transported over long distances. In soil, antimony is strongly associated with particles containing iron, manganese or aluminum. In water it usually adheres to sediments [9].

The determination of trace elements in sediment is particularly difficult because of the complexity of the matrix. The total analyte concentration can only be determined after a fusion with sodium carbonate [10], lithium tetraborate [11] or lithium metaborate [12–14], or after acid digestion in the presence of hydrofluoric acid and frequently also perchloric acid [15,16]. These digestion procedures are relatively time-consuming and certainly not without problems. The high reagent concentration requires regular blank controls to be performed, and frequently the calibration solutions have to be matched to the matrix content. Moreover

* Corresponding author at: Departamento de Química, Universidade Federal de Santa Catarina, 88040-900 Florianópolis - SC, Brazil. Tel.: +55 48 9983 1344; fax: +55 48 3721 6850.
E-mail address: welz@qmc.ufsc.br (B. Welz).
[1] www.inct.cienam.ufba.br.

0039-9140/$ – see front matter © 2009 Elsevier B.V. All rights reserved.
doi:10.1016/j.talanta.2009.08.004

the high salt concentration can lead to interferences in the final determination. Digestions in hydrofluoric or perchloric acid are dangerous, and next to silicon, which should be removed in this manner, a number of elements, including antimony, form volatile fluorides which might be lost during sample preparation.

Owing to these problems, instead of a total digestion or fusion, it is common in environmental analysis to use a leaching with *aqua regia* [17,18]. This method is based on the assumption that heavy metals that are so strongly bound to the mineral matrix that they do not go into solution under these conditions will also not be taken up by plants and cannot be dissolved by water or bacteria. Even if this assumption might be true for many elements and matrices, such an extraction cannot replace a determination of the total content of an analyte in all situations. In addition, the resulting matrix can cause serious interferences in most spectrometric techniques unless the solutions are strongly diluted, which is often not possible in trace element determinations, or the analyte is extracted, which is another time-consuming procedure.

Due to the difficulties of bringing environmental samples, such as sediments, into solution and due to the complexity of the resulting solutions, which might need additional treatment before they can be analyzed, direct solid sampling (SS) using electrothermal atomic absorption spectrometry with a graphite tube furnace (GF AAS) might be an attractive alternative [19]. However, the complex and refractory matrix of sediments might also cause problems in SS-GF AAS. Although non-spectral interferences can usually be controlled using the Stabilized Temperature Platform Furnace (STPF) concept [20], spectral interferences and the limited background correction capability of conventional line source atomic absorption spectrometers might be the major obstacle in the application of this technique [21]. The introduction of high-resolution continuum source AAS (HR-CS AAS) has brought about a significant change in this direction due to its unsurpassed background correction capabilities [22]. It has been demonstrated that a number of trace elements in a wide variety of complex sample matrices can be determined by SS-HR-CS GF AAS using aqueous standards for calibration, i.e., without any interference [23].

Chemical modifiers are routinely used in GF AAS as part of the STPF concept in order to thermally stabilize volatile analytes and enable the use of higher pyrolysis temperatures to remove the majority of the matrix prior to the atomization stage [24]. In SS-GF AAS the addition of a modifier in solution over the solid sample prior to every determination obviously complicates the procedure. Permanent chemical modifiers, which are usually applied as kind of a surface coating on the SS platform, have therefore been investigated intensively and have been shown to stabilize the analyte in a similar way as when it is applied in solution [25–29]. The mechanism of operation is believed to be a migration of the analyte to the modifier in the pyrolysis stage, as it has been demonstrated that the analyte is released from the sample well below its melting point [30]. Platinum group metals, mainly those with high melting points, i.e., Rh, Ru and Ir, have typically been used as permanent modifiers for the stabilization of volatile elements. The use of permanent modifiers also reduces blank values, as the modifier is purified during its thermal deposition, resulting in better limits of detection and quantification [17].

The goal of this work has been to develop a fast routine procedure for the determination of total antimony in sediments using SS-HR-CS GF AAS. The visibility of the spectral environment at high resolution in HR-CS AAS has also been used as a diagnostic tool in order to investigate spectral interferences that might impede the determination of antimony in sediment using conventional line source GF AAS. The investigation of permanent chemical modifiers has been included in the study for obvious reasons in order to simplify the procedure.

2. Experimental part

2.1. Instrumentation

All experiments were carried out with a prototype high-resolution continuum source atomic absorption spectrometer, built at ISAS Berlin, based on an AAS 6 Vario (Analytik Jena AG, Jena, Germany), from which the entire optical compartment, including detector and associated controls, was removed and replaced by a double monochromator, similar to that described by Heitmann et al. [31]. This monochromator consists of a pre-dispersing prism monochromator and an echelle grating monochromator, both in Littrow mounting, resulting in a spectral resolution of $\lambda/\lambda\Delta \approx 140\,000$. A xenon short-arc lamp XBO 301 (GLE, Berlin, Germany) with a nominal power of 300 W, operating in a *hot-spot* mode, was used as the continuum radiation source. A UV-sensitive charge coupled device (CCD) detector, model S7031-0906 (Hamamatsu Photonics, Japan), with 512×58 pixels operating in full vertical binning mode was used, resulting in a spectral bandwidth per pixel of about 2 pm at 231.147 nm. 200 pixels are used for analytical purposes, which corresponds to a spectral environment of about ±0.20 nm around the center pixel. Details of this equipment and its specific features have been described previously [22,32]. Atomic absorption has been measured at the secondary resonance line of antimony at 231.147 nm, which is about a factor of 2.4 less sensitive than the primary resonance line at 217.581 nm. Three pixels have been used for signal evaluation, corresponding to a spectral interval of ~6 pm, as the best signal-to-noise ratio has been obtained under these conditions. The absorbance values obtained this way are denominated Peak Volume Selected Absorbance (PVSA, $A_{\Sigma 3,\mathrm{int}}$), i.e., the integrated absorbance summated over three pixels [33]. The integrated absorbance values obtained with direct solid sampling have been normalized for 1.0 mg of sample, as it is impossible and unnecessary to weigh always the same sample mass.

The conventional transversely heated graphite tube atomizer supplied by Analytik Jena together with the AAS 6 Vario has been used throughout. All experiments were carried out using pyrolytically coated SS graphite tubes without a dosing hole (Analytik Jena, Part No. 07-8130325) and SS graphite platforms (Analytik Jena, Part No. 407-A81.312). Samples were weighed on a M2P microbalance (Sartorius, Göttingen, Germany) directly onto the SS platforms and inserted into the graphite tube using a pre-adjusted pair of tweezers, which is part of the SSA 5 accessory for manual SS (Analytik Jena). Argon 99.996% (White Martins, São Paulo, Brazil) was used as purge and protective gas. The temperature program adopted for aqueous standards (calibration) and for solid samples is shown in Table 1. In all figures in which time-resolved absorbance is shown,

Table 1
Graphite furnace temperature program for the determination of Sb in sediment samples by SS-HR-CS GF AAS using Ir as a permanent modifier.

Program stage	Temperature (°C)	Ramp (°C s^{-1})	Hold (s)
Drying 1	90	10	10
Drying 2	130	5	5
Pyrolysis	1100	50	15
Auto Zero[a]	1100	0	1
Atomization[a]	2100	3000	7
Cleaning	2500	1000	5

[a] Purge gas (argon) flow rate 2 L min^{-1} in all stages, except during Auto Zero and atomization, where the gas flow was interrupted.

Table 2
Graphite furnace temperature program for the deposition of iridium as a permanent modifier on the SS graphite platform.

Step	Temperature (°C)	Ramp (°C s^{-1})	Hold (s)
1	130	10	40
2	160	10	50
3	1000	20	25
4	1400	100	5
5	2000	100	5

recording starts with the 'Auto Zero' stage, i.e., 1 s prior to the atomization stage.

2.2. Reagents and samples

Analytical grade reagents were used throughout. The nitric acid 65% (Merck, Germany), used to prepare aqueous calibration standards, was further purified by sub-boiling distillation in a quartz apparatus (Kürner Analysentechnik, Rosenheim, Germany). Distilled, deionized water with a resistivity of 18 MΩ cm from a Milli-Q water purification system (Millipore, Bedford, MA, USA) was used for the preparation of aqueous calibration standards. The antimony stock solution was prepared from Sb_2O_3 (SPEX, Edison, NJ, USA). Iridium stock solution with 1000 mg L^{-1} Ir in 1 mol L^{-1} nitric acid (Fluka, Buchs, Switzerland) was used as provided for coating of the platform.

The following certified reference materials (CRM) were used for validation of the method: NIST SRM 8704 (Buffalo River Sediment), NIST SRM 2702 (Inorganics in Marine Sediment), NIST SRM 2703 (Sediment for Solid Sampling Analytical Techniques) and NIST SRM 1646a (Esturine Sediment) (all from National Institute of Standards and Technology, Gaithersburg, MD, USA); Marine Sediment MESS-3, HISS-1 and PACS-2 from National Research Council of Canada (NRCC, Ottawa, Canada).

2.3. Procedure

Iridium was thermally deposited onto the platform surface using 10 repetitive injections of 40 μL of the 1000 mg L^{-1} Ir stock solution as described previously [34]. After each injection, the temperature program shown in Table 2 was applied. One coating has been sufficient for the lifetime of a SS platform. For the determination of Sb, sediment samples were ground in an agate mortar and passed through a polyester sieve for particle size <50 μm. Aliquots containing between 0.02 and 1.1 mg were weighed directly onto the SS platforms and inserted into the graphite tube with the SSA 5 accessory. Calibration solutions (20 μL) were injected manually onto the SS platforms using a micro-pipette. The analysis of one sample including five repetitive weighings and determinations takes less than 10 min, making possible the analysis of about 50 samples per working day.

3. Results and discussion

3.1. Pyrolysis and atomization temperatures

All method development and optimization experiments were carried out using an aqueous standard and NIST SRM 8704 (Buffalo River Sediment). Fig. 1 shows the pyrolysis curves obtained for the sediment CRM (Fig. 1a) and the aqueous standard (Fig. 1b) without a modifier and with iridium as a permanent modifier. Without a modifier antimony is partially lost above 800 °C from the aqueous standard and above 900 °C from the sediment CRM. In the presence of the permanent modifier a pyrolysis of 1100 °C can be used for the sediment, and an even higher pyrolysis temperature would be possible for the aqueous standard. A pyrolysis temperature of 1100 °C has been selected for all further experiments. The atomization temperature has been optimized in a similar way considering sensitivity and signal shape, and a temperature of 2100 °C has finally been selected.

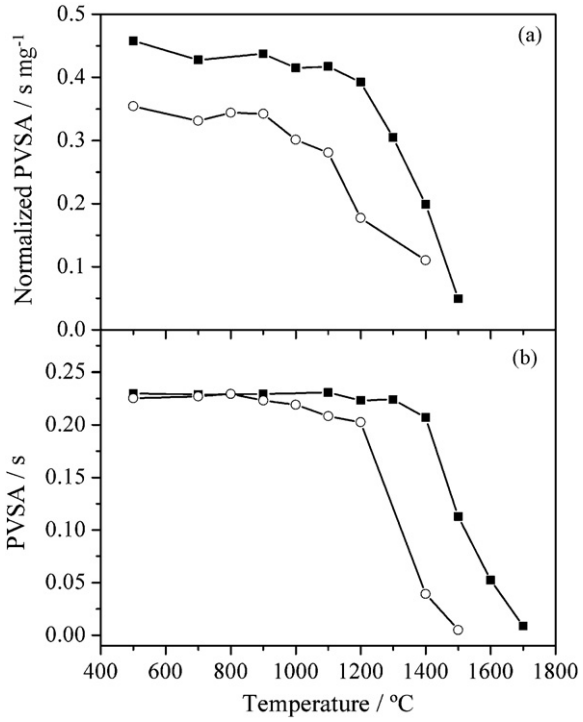

Fig. 1. Pyrolysis curves for Sb –○– without modifier and –■– with 400 μg Ir as permanent modifier; atomization temperature: 2100 °C; (a) NIST SRM 8704 (Buffalo River Sediment), PVSA ($A_{\Sigma 3,int}$) normalized for 1 mg of sample; (b) aqueous standard containing 1.3 ng Sb in 0.5% (v/v) HNO_3.

3.2. Background absorption and background correction

In HR-CS AAS 'continuous' background absorption, i.e., background absorption that does not exhibit any fine structure within the spectral range that is probed by the detector, such as radiation scattering or molecular absorption due to dissociation continua or polyatomic molecules, is corrected automatically and simultaneously with the measurement of atomic absorption using correction pixels. After this correction only discontinuous absorption, such as atomic absorption and molecular absorption due to diatomic molecules, which exhibits pronounced fine structure that can be resolved by the spectrometer, is displayed by the equipment.

The time- and wavelength-resolved absorption spectrum obtained for NIST SRM 8704 (Buffalo River Sediment) in the vicinity of the antimony line at 231.147 nm after automatic correction for continuous background is shown in Fig. 2. The Sb atomic absorption line and a secondary absorption line of Fe at 231.31 nm are marked with arrows; all the other lines are part of an electronic transition spectrum of one or more diatomic molecule(s) with pronounced rotational fine structure. There are actually three different phases within the time frame of the atomization stage. The first one is the appearance of very sharp peaks of a rotational fine structure at the onset of the atomization stage; the second set of molecular bands appears more or less together with the atomic absorption of Sb (and Fe), but does not return to the baseline; instead, towards the end of the atomization cycle, the molecular absorption increases rapidly to relatively high absorbance values. Due to the post-processing capability of the spectrometer it is possible to analyze the recorded spectrum after it has been stored in the computer in order to iden-

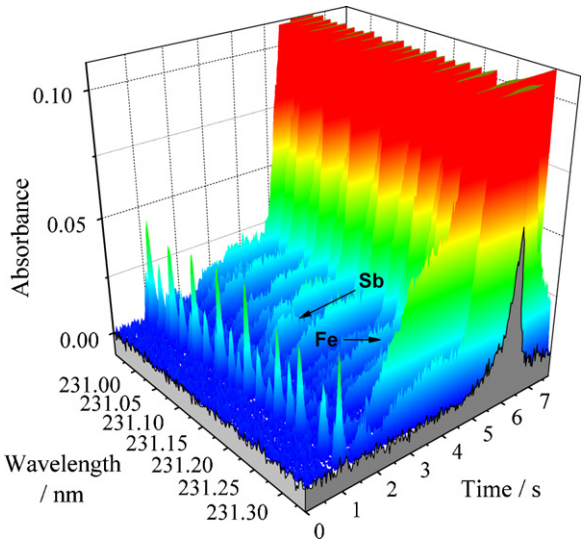

Fig. 2. Time- and wavelength-resolved absorbance spectrum recorded for NIST SRM 8704 (Buffalo River Sediment) in the vicinity of the Sb line at 231.147 nm after automatic correction for continuous background absorption; T_{pyr} = 1100 °C; T_{at} = 2100 °C; Ir as permanent modifier.

tify the molecular structures and to correct them using reference spectra and a least-squares algorithm [22].

Fig. 3a–c shows the three phases as wavelength-resolved absorbance spectra integrated over three time intervals, i.e., from 0 to 1.4 s, which are the first 0.4 s of the atomization stage, as signal recording starts with the Auto Zero stage (Fig. 3a); from 1.4 to

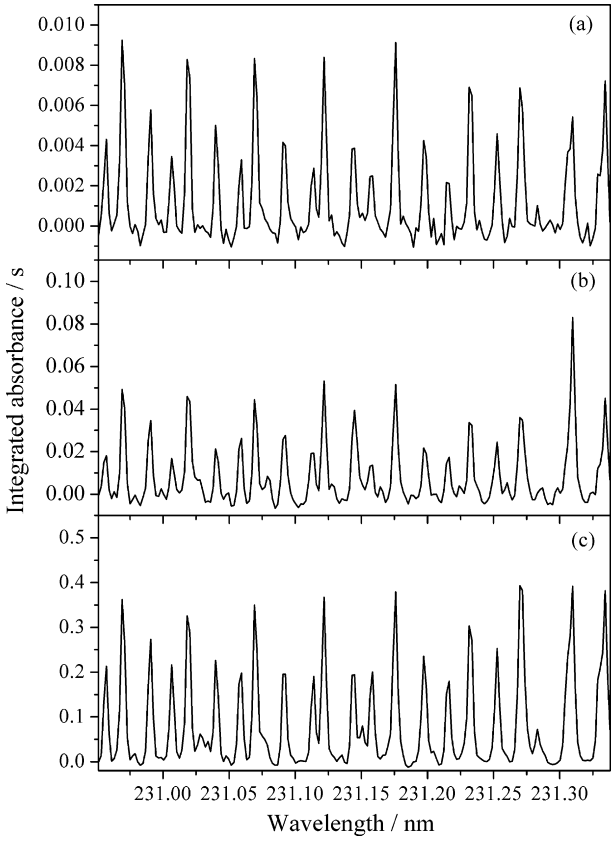

Fig. 3. Wavelength-resolved integrated absorbance spectrum in the vicinity of the Sb line at 231.147 nm for 0.092 mg of NIST SRM 8704 (Buffalo River Sediment); Ir as permanent modifier; T_{pyr} = 1100 °C; T_{at} = 2100 °C; (a) integration limits 0.0–1.4 s; (b) integration limits 1.4–4.2 s; (c) integration limits 4.2–7.0 s.

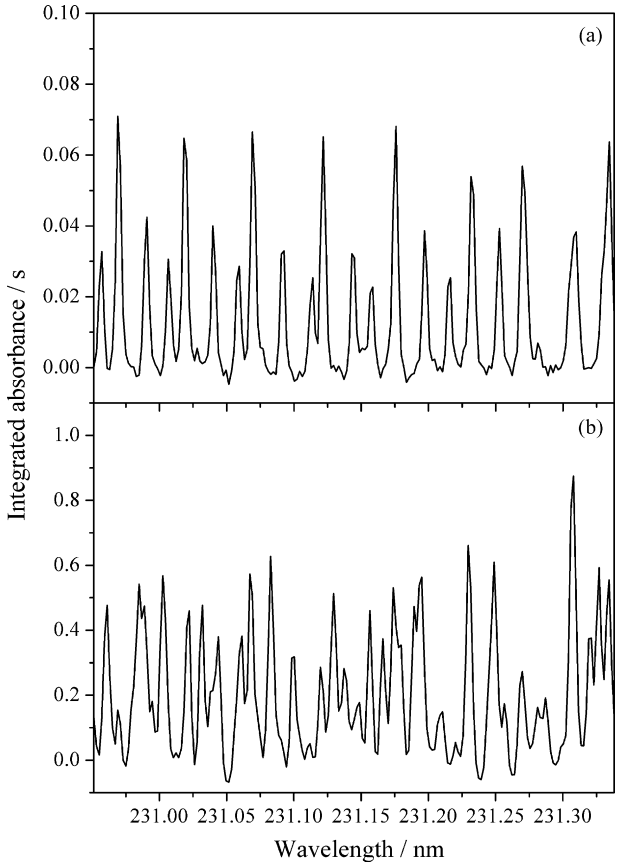

Fig. 4. Wavelength-resolved integrated absorbance spectrum in the vicinity of the Sb line at 231.147 nm; Ir as permanent modifier; T_{pyr} = 1100 °C; T_{at} = 2100 °C; (a) 0.116 mg of silica; (b) 150 μg P as $NH_4H_2PO_4$.

4.2 s, which is the period in time when the Sb atomic absorption signal appears (Fig. 3b); and from 4.2 to 7.0 s, which is the period after the Sb absorption signal returned to the baseline and the molecular absorption reaches fairly high levels (Fig. 3c). Although the spectra appear to be similar, they are not exactly identical. For this reason two reference spectra have been recorded, one for the silicon monoxide SiO, using pure silica (SiO_2), and one for the phosphorus monoxide PO, using ammonium dihydrogen phosphate ($NH_4H_2PO_4$), which are shown in Fig. 4a and b, respectively. The spectrum recorded for HISS-1 CRM, which has a very low antimony content (information value: 0.13 μg g^{-1}), has also been used for correction purposes in some cases, but is not shown here, as it is almost identical to that of SiO (Fig. 4a).

The spectrum shown in Fig. 3a, which appears at the onset of the atomization stage, has been identified as being exclusively due to SiO, and could be corrected to the baseline using the reference spectrum in Fig. 4a and least-squares background correction (LSBC). This is actually surprising, as this means that there is a silicon-containing compound in the sediment that is significantly more volatile than antimony, i.e., it cannot be mineral SiO_2; this early SiO absorption spectrum has been observed in all investigated sediment CRM. The molecular structures of the spectrum shown in Fig. 3b, which actually comprises the main atomization stage, could be removed reasonably well using LSBC and the spectrum of HISS-1 or SiO as reference spectrum; however, as can be seen in Fig. 5a, besides the atomic absorption peaks of antimony and iron, there are some irregularities in the baseline, indicating some correction problems, most likely due to a small amount of another diatomic molecule. Nevertheless, as these minor irregularities did not affect the analytical line, and were less than ±0.01 s in integrated absorbance,

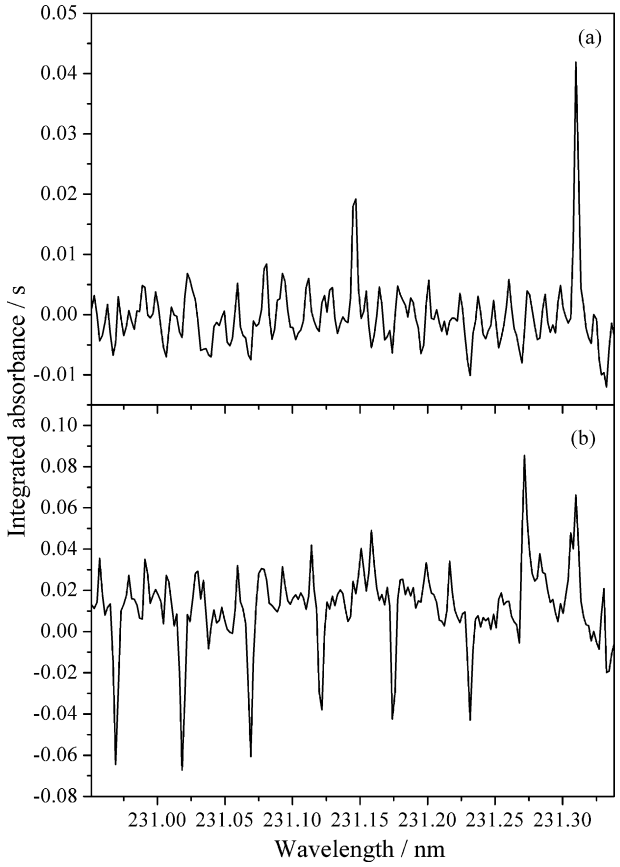

Fig. 5. Wavelength-resolved integrated absorbance spectrum in the vicinity of the Sb line at 231.147 nm for 0.092 mg of NIST SRM 8704 (Buffalo River Sediment) using HISS-1 CRM as reference spectrum for LSBC; Ir as permanent modifier; T_{pyr} = 1100 °C; T_{at} = 2100 °C; (a) integration limits 1.4–4.2 s; (b) integration limits 4.2–7.0 s.

they have not been further investigated. The third section of the absorption spectrum, which is shown in Fig. 3c, is of no analytical interest, as it occurs in time after the atomization of antimony, but it might be of diagnostic interest in order to find out the source of this molecular absorption. A first attempt to correct for this molecular absorption using the spectrum of HISS-1 as a reference failed at least in part, as can be seen in Fig. 5b. There was a baseline offset of about 0.015 s in integrated absorbance, and pronounced negative peaks that coincided with the strongest absorption lines of SiO. The explanation for this phenomenon is straight-forward when we compare Fig. 3c with a maximum absorbance of about 0.4 s and Fig. 4a, where the maximum absorbance only reaches values of about 0.07 s. The intensity ratio between the strongest and the less intense absorption peaks in Fig. 4a is roughly 2:1, whereas in Fig. 3c it is less, indicating that the absorbance of the strongest peaks is already in the non-linear range, a task that cannot be solved by a least-squares algorithm.

This situation has therefore been investigated in more detail, primarily in the environment of the analytical line. Fig. 6 shows the absorbance signal over time recorded at the central pixel at 231.147 nm for the NIST SRM 8704 (Buffalo River Sediment) using different reference spectra for correction. Without LSBC there appears a strong molecular absorption after the antimony signal, which can only be corrected in part using the spectrum of HISS-1 CRM. The correction is much better using the reference spectrum of SiO, but there is still a residual signal that could only be corrected using the reference spectrum of PO in addition to that of SiO. This also explains why the spectrum of the HISS-1 CRM could not be used successfully for LSBC, at least not in this time interval. When-

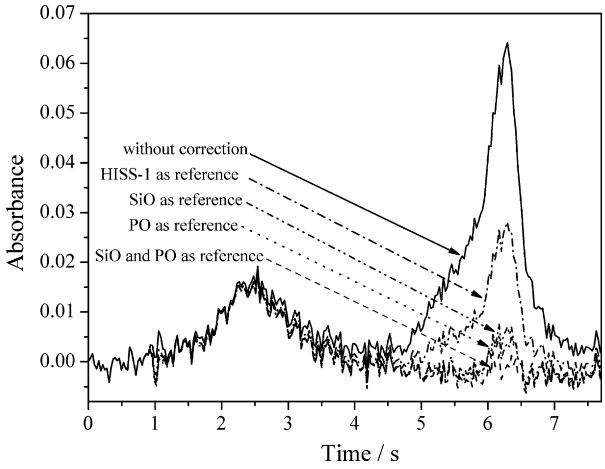

Fig. 6. Superimposed transient signals recorded at 231.147 nm for NIST SRM 8704 (Buffalo River Sediment) without LSBC (black line) and using the spectrum of HISS-1, SiO, PO, and SiO + PO, as reference for LSBC.

ever more than one molecule is contributing to such a spectrum, the reference spectra and the LSBC have to be applied sequentially for each molecule, unless the ratio between the two molecules is known and can be simulated in the reference spectrum, which is impossible in real sample analysis.

Obviously, this correction appears to be of no importance for the analyte signal, which returns to the baseline before the molecular absorption becomes significant. However, Fig. 6 only shows the situation at the central pixel, whereas the best S/N ratio is obtained using PVSA over three pixels; the results obtained for NIST SRM 8704 using this evaluation technique are shown in Table 3. It is obvious that a wrong result is obtained without using LSBC, as one of the rotational lines of the SiO molecular absorption is already overlapping significantly with the wing of the antimony absorption line. On the other hand there is little difference in the final result if HISS-1 is used for correction or SiO alone or together with PO, indicating the robustness of the method. The use of PO alone for LSBC does not give a satisfactory result, showing that this molecule has no significant contribution to the absorption spectrum during the first 4.2 s of the atomization stage. The fact that some correction has been achieved even with PO as the reference spectrum is due to some similarity of this spectrum with that of SiO (see Fig. 4a and b). The LSBC has therefore been in part successful to correct for the effect of SiO on the integrated absorbance of Sb using the spectrum of PO, although the final result is not within the confidence interval.

As a result of these investigations it would be of advantage to shorten the atomization stage to about 4 s in order to avoid the strong molecular absorption at the end of the atomization stage and remove these matrix components during the cleaning stage. A typical time- and wavelength-resolved absorbance spectrum recorded under these conditions, using LSBC for SiO and PO is shown in Fig. 7.

Table 3
Results obtained for antimony in NIST SRM 8704 (Buffalo River Sediment) (certified value: 3.07 ± 0.32 μg g^{-1} Sb) using different reference spectra for LSBC; integration interval: 0.5–4.5 s; T_{pyr} = 1100 °C; T_{at} = 2100 °C; Ir as permanent modifier.

Reference spectrum	Found value (μg g^{-1})[a]	Recovery (%)[b]
Without LSBC	4.61 ± 1.37	150 ± 35
HISS-1	2.96 ± 0.29	96 ± 9
SiO	2.77 ± 0.42	90 ± 14
PO	3.58 ± 0.86	117 ± 28
SiO + PO	2.81 ± 0.46	91 ± 15

[a] Average of five determinations ± confidence interval (at the 95% level).
[b] Recovery factor = (found value/certified value) × 100 ± confidence interval.

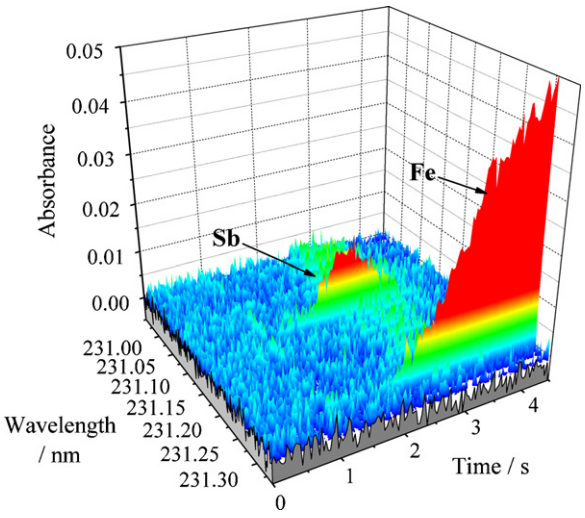

Fig. 7. Time- and wavelength-resolved absorbance spectrum recorded for 0.092 mg of NIST SRM 8704 (Buffalo River Sediment) in the vicinity of the Sb line at 231.147 nm after correction for continuous and discontinuous background absorption using the reference spectra of SiO and PO for LSBC; Ir as permanent modifier; T_{pyr} = 1100 °C; T_{at} = 2100 °C; integration interval: 0–4.5 s.

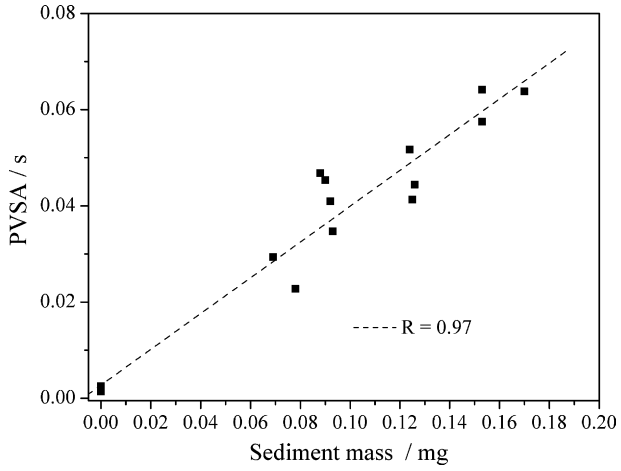

Fig. 8. Correlation between the sediment mass (NIST SRM 8704, Buffalo River Sediment) introduced into the graphite furnace and the PVSA ($A_{\Sigma 3,int}$); T_{pyr} = 1100 °C; T_{at} = 2100 °C; Ir as permanent modifier.

In essence only the analyte signal and the atomic absorption due to Fe are visible under these conditions.

3.3. Figures of merit

The limit of detection (LOD) has been calculated as three times the standard deviation of 10 measurements of a blank divided by the slope of the calibration curve; in SS-GF AAS the blank measurements are usually carried out according to the "zero mass response" technique [35], introducing repeatedly an SS platform containing only the modifier and running a full atomization cycle. The limit of quantification (LOQ) is based on the same measurements, using 10 times the standard deviation of the blank readings. The LOD and LOQ were determined as 0.02 and 0.07 μg g^{-1} Sb, respectively, based on a sample mass of 0.2 mg introduced into the furnace. A larger sample mass could obviously be introduced, resulting in even lower LOD and LOQ; however this was not found necessary for the present investigation. The characteristic mass (m_0), defined as the mass of the analyte that produces a PVSA of 0.0044 s, has been determined as m_0 = 28 pg Sb. There is no literature data available for the characteristic mass for the secondary Sb line at 231.147 nm used in this work. The characteristic mass at the main resonance line for Sb at 217.58 nm using line source AAS is around m_0 = 20 pg, and the secondary line used in this work is about a factor of 2.4 less sensitive than the primary resonance line [24], which would result in a characteristic mass of about 48 pg; it is quite typical for HR-CS AAS that the sensitivity obtained with PVSA is better than that obtained with line source AAS. A calibration curve established using a blank and six calibration solutions in the concentration range 5–50 μg L^{-1} Sb (mass range: 100–1000 pg Sb) in 0.007 mol L^{-1} HNO_3, using the conditions described in Section 2 gave the linear relationship:

$$A_{\Sigma 3,int} = 1.55 \times 10^{-4} m + 0.00002 \quad (R = 0.9998),$$

where $A_{\Sigma 3,int}$ is the PVSA, i.e., the integrated absorbance summated over three pixels, and m is the analyte mass.

3.4. Accuracy, precision and analytical application

The correlation between the sediment mass introduced into the graphite furnace and the integrated absorbance (PVSA, $A_{\Sigma 3,int}$) for NIST SRM 8704 is shown in Fig. 8. The sample mass has been varied in the range from 0.069 ± 0.001 to 0.170 ± 0.001 mg; each measurement point corresponds to an individual sample weighing and measurement, and is hence an indication for the precision of the entire procedure, which will be discussed in some more detail later. The good linear correlation shows that at least up to about 0.2 mg of sediment sample can be introduced and measured with the proposed procedure.

Six sediment CRM (one river, one estuarine and four marine sediments) have been analyzed; each concentration value was obtained as the mean of five individual weighings and measurements, using a calibration curve established with aqueous standards for quantification. The results are shown in Table 4 together with the calculated recovery and uncertainty (95% confidence interval). There is no statistically significant difference between the results obtained with the proposed method and the certified or informed values based on a Student's t-test ($t_{calculated}$ = 0.93; t_{value} = 2.57, n = 6). These results show that the determination of antimony in sediment using SS-HR-CS GF AAS can be carried out with calibration against aqueous standards.

The precision, expressed as relative standard deviation (% RSD), ranged between 7% and 17%, which are typical values for the direct analysis of solid samples. Although these values should not be over-interpreted, it might be interesting to note that the highest imprecision has been obtained for the sample with the highest antimony content, and the best precision for a sample with about an order of magnitude lower antimony content. As smaller sample masses are usually introduced into the furnace for samples with high analyte content, this difference in precision might be

Table 4
Results obtained for the determination of antimony in sediment samples using SS-HR-CS GF AAS and calibration against aqueous standards; T_{pyr} = 1100 °C; T_{at} = 2100 °C; Ir as permanent modifier.

CRM	Certified value (μg g^{-1})	Found value (μg g^{-1})[a]	Recovery (%)[b]
NIST SRM 8704	3.07 ± 0.32	2.96 ± 0.29	96 ± 9
PACS-2	11.6 ± 2.6	12.6 ± 2.0	109 ± 17
MESS-3	1.02 ± 0.9	0.98 ± 0.07	96 ± 7
NIST SRM 2703	5.62 ± 0.26	5.80 ± 0.67	103 ± 12
NIST SRM 2702	5.60 ± 0.24	5.49 ± 0.68	98 ± 12
NIST SRM 1646a[c]	0.40	0.45 ± 0.05	113 ± 13

[a] Average of five determinations ± confidence interval (at the 95% level).
[b] Recovery factor = (found value/certified value) × 100 ± confidence interval.
[c] Informed value, not certified.

directly related to the sample mass and the natural inhomogeneity of samples such as sediments. Another interesting comparison is that between NIST SRM 2702 and 2703, which are actually the same CRM, with the only difference that the latter one is ground to smaller particle size. The fact that the same imprecision has been obtained for both CRM might suggest that particle size is not of decisive importance for SS-GF AAS, as was proposed by others previously [36].

4. Conclusion

A simple, fast and reliable method for the determination of antimony in sediment has been developed using direct solid sampling HR-CS GF AAS and calibration against aqueous standards, i.e., without interference. As the spectral environment of the analytical line becomes visible at high resolution with this technique, it is possible to draw some conclusion about the performance of conventional line source AAS in the analysis of these samples. Spectrometers with deuterium or similar continuum source background correction are unable to cope with this background, which appears in time together with the analyte signal; as this kind of correction system makes an average of the background over the spectral band pass, background correction errors are inevitable. The same is true for Smith–Hieftje background correction, which measures the background on both sides of the analytical line, which is in this case obviously not the same as on the analytical line. To which extent Zeeman-effect background correction could deal with this spectral situation is difficult to predict; however, it is known that the narrow rotational lines of various diatomic molecules also exhibit Zeeman splitting. This would mean that the background measured with magnetic field is not identical to that without magnetic field, which would result in a correction error. The extent of this error could obviously only be determined by experiment. Nevertheless, the background correction systems available with HR-CS AAS are far superior to those available for line source AAS, and it might be expected that a variety of other trace elements could be determined in sediment and similar materials without interference using this technique. In addition, with modern equipment, in contrast to the prototype used in this work, full automation of direct solid sampling analysis is possible, which is obviously of importance for routine analysis.

Acknowledgements

The authors are grateful to Conselho Nacional de Desenvolvimento Científico and Tecnológico (CNPq) for financial support. R.G.O.A., B.W. and F.V. have research scholarships from CNPq. The authors are also grateful to Analytik Jena for financial support and donation of the prototype high-resolution continuum source atomic absorption spectrometer.

References

[1] J.L.G. Ariza, E. Morales, D. Sanchez-Rodas, I. Giraldez, Trends Anal. Chem. 19 (2000) 200.
[2] K. Müller, B. Daus, P. Morgenstern, R. Wennrich, Water Air Soil Poll. 183 (2007) 427.
[3] W. Shotyk, M. Krachler, B. Chen, in: A. Sigel, H. Sigel, R.K.O. Sigel (Eds.), Metal Ions in Biological Systems, vol. 44, M. Dekker, New York, 2005, p. 172.
[4] P. Smichowski, Talanta 75 (2008) 2.
[5] J.M. Carlosena, M.L. Andrade, S. Martínez, P.L. Muniategui, D. Prada, M.J. Cal-Prietro, Water Air Soil Poll. 129 (2001) 333.
[6] Toxicological Profile for Antimony, U.S. Department of Health and Human Services, Public Health Service, Agency for Toxic Substances and Disease Registry, Atlanta, GA, USA, 1992.
[7] E.V. Bogdanov, V.V. Vladimirov, V.N. Gorshkov, Solid State Comm. 46 (1983) 193.
[8] United Nations Environment Programme, International Labour Organization, World health Organization, Environmental Health Criteria 192, Flame Retardants: A General Introduction. http://www.inchem.org/documents/ehc/ehc/ehc192.htm (accessed July 2009).
[9] Antimony and Compounds Fact Sheet, Australian Government. http://www.npi.gov.au/database/substance-info/profiles/10.html#npi-rank (accessed July 2009).
[10] P.J. Potts, Handbook of Silicate Rocks Analysis, Blackie & Sons, Glasgow, 1987.
[11] E.A.H. Carballo, J.R. Domínguez, J. Alvarado, Atom. Spectrosc. 21 (2000) 132.
[12] D.C. Bartenfelder, A.D. Karathanasis, Commun. Soil. Sci. Plant 19 (1988) 471.
[13] M. Bettinelli, Anal. Chim. Acta 148 (1983) 193.
[14] A.A. Verbeek, M.C. Mitchell, A.M. Ure, Anal. Chim. Acta 135 (1982) 215.
[15] H. Agemian, E. Bedek, Anal. Chim. Acta 119 (1980) 323.
[16] P. Woitke, A. Thiesies, G. Henrion, G. Steppuhn, Z. Chem. 29 (1989) 180.
[17] J.B.B. da Silva, M.A.M. da Silva, A.J. Curtius, B. Welz, J. Anal. At. Spectrom. 14 (1999) 1737.
[18] M. Chen, L.Q. Ma, Soil Sci. Soc. Am. J. 65 (2001) 491.
[19] M.G.R. Vale, N. Oleszczuk, W.N.L. dos Santos, Appl. Spectrosc. Rev. 41 (2006) 377.
[20] W. Slavin, D.C. Manning, G.R. Carnrick, Atom. Spectrosc. 2 (1981) 137.
[21] M.G.R. Vale, B. Welz, Spectrochim. Acta Part B 57 (2002) 1821.
[22] B. Welz, H. Becker-Ross, S. Florek, U. Heitmann, High-resolution Continuum Source AAS—The Better Way to Do Atomic Absorption Spectrometry, Wiley–VCH, Weinheim, 2005.
[23] B. Welz, M.G.R. Vale, D.L.G. Borges, U. Heitmann, Anal. Bioanal. Chem. 389 (2007) 2085.
[24] B. Welz, M. Sperling, Atomic Absorption Spectrometry, 3rd edn, Wiley–VCH, Weinheim, 1999.
[25] M.G.R. Vale, M.M. Silva, B. Welz, E.C. Lima, Spectrochim. Acta Part B 56 (2001) 1859.
[26] M.G.R. Vale, M.M. Silva, B. Welz, R. Nowka, J. Anal. At. Spectrom. 17 (2002) 38.
[27] A.F. Silva, B. Welz, A.J. Curtius, Spectrochim. Acta Part B 57 (2002) 2031.
[28] A.F. Silva, D.L.G. Borges, F.G. Lepri, B. Welz, A.J. Curtius, U. Heitmann, Anal. Bioanal. Chem. 382 (2005) 1835.
[29] D.L.G. Borges, A.F. Silva, B. Welz, A.J. Curtius, U. Heitmann, J. Anal. At. Spectrom. 21 (2006) 763.
[30] O.A. Güell, J.A. Holcombe, J. Anal. At. Spectrom. 7 (1992) 135.
[31] U. Heitmann, M. Schütz, H. Becker-Ross, S. Florek, Spectrochim. Acta Part B 51 (1996) 1095.
[32] B. Welz, D.L.G. Borges, F.G. Lepri, M.G.R. Vale, U. Heitmann, Spectrochim. Acta Part B 62 (2007) 873.
[33] U. Heitmann, B. Welz, D.L.G. Borges, F.G. Lepri, Spectrochim. Acta Part B 62 (2007) 1222.
[34] A.F. da Silva, D.L.G. Borges, F.G. Lepri, B. Welz, A.J. Curtius, U. Heitmann, Anal. Bioanal. Chem. 382 (2005) 1835.
[35] U. Kurfürst, in: U. Kurfürst (Ed.), Solid Sample Analysis, Springer, Heidelberg, 1998, p. 21.
[36] M.A. Belarra, M. Resano, J.R. Castillo, J. Anal. At. Spectrom. 13 (1998) 489.